

## IMPACT OF TRANSONIC COMPRESSOR ROTOR LEADING EDGE SHAPE ON THE SHOCK STRUCTURE NEAR THE CASING

Martin Hoeger  
MTU Aero Engines  
Dachauerstr. 665  
D-80995 Munich, Germany  
+49 (0)89 1489 6175  
Martin.Hoeger@muc.mtu.de

Martin Engber  
MTU Aero Engines  
Dachauerstr. 665  
D-80995 Munich, Germany  
+49 (0)89 1489 9074  
Martin.Engber@muc.mtu.de

Jörg Bergner  
Darmstadt University of Technology  
Petersenstr. 30  
D-64287 Darmstadt, Germany  
+49 (0)6165 16 4159  
bergner@gfa.tu-darmstadt.de

### ABSTRACT

The efficiency of a transonic compressor rotor is known to depend by a large amount on the flow at the rotor tip and on the way the flow interacts with the shock system at the casing. To further extend off-design capability and loading limits, several compressor rotors have been investigated at the *single stage transonic compressor rig* at Darmstadt University of Technology. The rotor leading edge shapes may be characterised by forward sweep, standard and backward sweep/ backward lean.

On the basis of 3D Navier-Stokes simulations the leading edge shape at the rotor tip is demonstrated to have a pronounced impact on the shock situation. A critical sweep angle may be deduced from the present investigations for backward swept rotor designs. The orientation of the passage shock at the casing is shown to depend not only on the tip leakage vortex and the way it displaces the undisturbed flow but also on the interaction of the bow shock at the leading edge with the casing. Close to the suction surface tip region for all rotors an approximately normal shock situation is found. For a backward swept rotor leading edge, however, the normal shock condition at the casing is demonstrated to be not only valid within the blade passage but more important, for the flow in front of the leading edge.

### INTRODUCTION

In the past the 3D design of compressor rotors has been studied by a large number of researchers. An overview on the development history of compressor blades made in Cybick and Hah (1997) clearly shows a trend towards low aspect ratio designs and forward swept blades. While low aspect ratios are understood to enable high stage loading, the forward swept blade was demonstrated by Hah et al. (1998) and Denton (1999) to promote stable and efficient

compressor designs. Here the blade shape is in line with the shock structure near the casing, where for all rotor designs an approximately normal shock situation is demonstrated to exist in radial direction. This finding is in conflict with backward swept rotor design idea, to reduce shock losses by creating an oblique shock system within the blade passage in the radial direction.

With the invention of new mechanical design strategies and advanced materials like carbon fiber reinforced plastic (CFRP), complex 3D blade shapes are made possible. A highly backward swept/ backward leaned rotor design was successfully tested at the *Axial Single-stage Transonic Compressor Rig* of TU Darmstadt, see Blaha et al. (2000). On the basis of numerical simulations for this rotor Bergner et al. (2002) studied the impact of lean on the shock structure in the blade passage. Since then at MTU Aero Engines several rotor design studies have been made for TU Darmstadt test rig, see e.g. Passrucker et al. (2003) for a forward swept design.

A careful evaluation of 3D Navier-Stokes predictions for all the design studies indicated the normal shock situation at the casing not only to be valid inside the blade passage but more important to exist for the bow shock in front of the leading edge too. In the present paper the impact of leading edge sweep angle on bow shock losses and shock structure close to the casing is investigated.

### NOMENCLATURE

*lean* circumferential lean, forward leaned with speed  
*sweep* axial sweep, backward swept with increasing axial co-ordinate  
 $Ma_1$  inlet Mach number relative frame  
 $P_t, P_{tr}$  total pressure in absolute, relative frame  
 $p$  static pressure  
 $r, y, x$  co-ordinates (radial, circumferential and axial)

- s streamwise co-ordinate  $s = x/\cos(\beta_{1x})$
- $\beta_{1x}$  inlet swirl angle in rel frame at the casing  
 $\beta_{1x} = \text{atan}(w_{1y}/w_{1x})$ , see fig. 1; (w velocity)
- $\beta_s$  stagger angle
- $\epsilon_{le}$  leading edge sweep angle in a streamsurface, see eqn. (1) and fig 1. (backward swept negative)
- $\epsilon_{sw}$  sweep angle defined by eqn. (1b)
- $\omega_{inl}$  loss coefficient inlet section, see eqn. (2)
- $\omega_{prof}$  loss coefficient profile section, see eqn. (3)
- l, le, te inlet plane, leading edge and trailing edge of rotor blade
- tip location at the outer casing

## ROTOR GEOMETRY

### Sweep angle definition

At the blade tip a sweep angle may be defined from the projection of the blade on a streamsurface constructed with the radial  $r$  and the streamwise direction  $s$  (average flow at rotor inlet), see Fig. 1. For the example of a backward swept, backward leaned rotor a small change in radial position  $\Delta r$  at the leading edge close to the tip is considered. With  $\Delta x$  and  $\Delta y$  as corresponding displacement in axial and circumferential direction, respectively, the leading edge sweep angle  $\epsilon_{le}$  in a streamsurface with constant inlet swirl angle  $\beta_{1x}$  may be defined by eqn. (1):

$$\epsilon_{le} = - \text{atan} ( (\Delta x \cos(\beta_{1x}) + \Delta y \sin(\beta_{1x}))/\Delta r ) \quad (1).$$

To be independent from flow conditions for the present investigations in eqn.(1) the swirl angle  $\beta_{1x}$  is substituted by the stagger angle at the tip for convenience:

$$\epsilon_{sw} = \epsilon_{le} (\beta_{1x} = \beta_{s,tip}) \quad (1b).$$

Eqn. (1b) is constructed for a casing geometry with constant radius. For compressor designs with contraction at the outer casing, eqn. (1b) may be extended easily by:

$$\epsilon_{sw,r} = \epsilon_{le} + \epsilon_{cas} \quad (1c),$$

with  $\epsilon_{cas} = \text{atan}((\Delta r/\Delta x)_{cas} \cdot \cos(\beta_{s,tip}))$ , where  $(\Delta r/\Delta x)_{cas}$  represents the slope of the casing in the meridional plane.

### Sweep Angle and Bow Shock

From eqn. (1b) follows that the leading edge sweep angle depends on both axial sweep and circumferential lean as well as on stagger (which for  $Ma_1 > 1$  is connected with design inlet flow angle). From leading edge bluntness and classical transonic compressor blade section design rules, see Schreiber (1988), it is assumed in the leading edge region the bow shock to be fairly attached and in a  $xy$ -plane normal to the inlet flow direction, see dashed plane

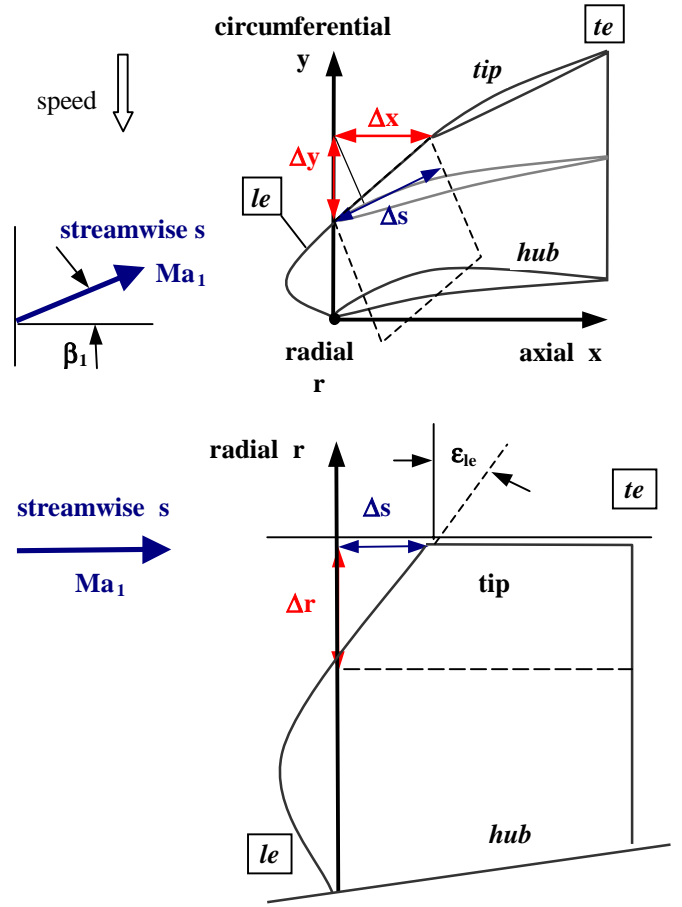


**Fig. 1: Leading edge effective sweep angle definition at the casing, radial view (top) and view normal to streamsurface (bottom)**

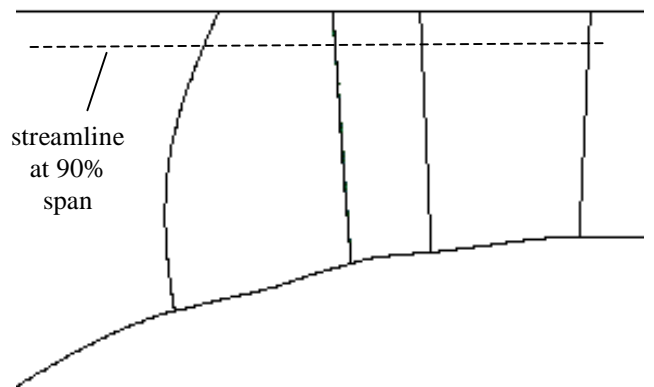


**Fig. 2: Meridional view of compressor stage with aft-swept rotor 2, representative streamline at 90% span (dashed line)**

Rotor No.	pressure ratio (stage)	Ma1 Rot tip	sweep angle $\alpha_{sw}$ [deg] rel to ref	aspect ratio	av. solidity	exp.	design method	design type
1	1.51	1.224	0	1	1.5	x	2D (S2, S1-Euler)	conv. stacked
2	1.49	1.216	-46	1.11	1.36	x	3D Euler + shear	bw sweep, bw lean
2a	1.48	1.223	-17	1.11	1.36	-	Rot 2 modified	bw sweep, no lean
2b	1.47	1.22	14	1.11	1.36	-	Rot 2 modified	bw sweep, fw lean
3	1.5	1.227	37	0.93	1.5	x	3D Navier-Stokes	fw sweep
4	1.5	1.227	18	0.99	1.5	-	3D Navier-Stokes	fw sweep

**Table 1: Geometry of Rotor designs investigated**

in Fig. 1, at the top. With this assumption the sweep angle  $\epsilon_{sw}$  may be regarded as a measure for the inclination of the shock wave in the streamwise direction. Eqn. (1b) is used together with eqn. (1) to judge the individual designs with respect to their ability in allowing for attached bow shocks at the tip. For basics on shock systems in compressor rotors the reader is referred to Bölcs and Suter (1985).

### Rotors Investigated

A total of 6 Rotor designs have been investigated of which 5 designs are already presented in publications with experimental data available for 3 designs. For all rotors the same stator vane is used. Inlet conditions, speed as well as stage pressure ratio was almost identical. Average geometrical parameters are given in Table 1, including sweep angles obtained from eqn. (1b) (average  $\epsilon_{sw}$  values 80 to 100% span). Main design parameters are found in Table 2:

design parameters	stage	
total pressure ratio	1.5	
Corrected mass flow rate	16 kg/s	
Inlet hub to tip ratio	0.51	
Corrected tip speed	398 m/s	
Ax. Mach No. in-/ outlet	0.48/ 0.49	
Flow/ work coefficient	0.60/ 0.81	
design parameters	rotor	stator
Max inlet Mach No.	1.34 (tip)	0.66 (hub)
Reynolds No.	$2.1 \cdot 10^6$	$0.7 \cdot 10^6$
Blade/ vane count	16	29

Table 2: Design parameters Single Stage Compressor Rig of TU Darmstadt , rotor No. 1.

From references given below further information on the aerodynamics of these designs may be obtained from:

Rot 1: Fritsch and Möhres (1997), Hoeger et al. (1998), Fritsch et al. (1997), Hoeger et al. (2000),

Rot 2: Blaha et al. (2000), Pirker and Frischbier (2002), Kablitz et al. (2002), Bergner et al. (2002)

Rot 2a: Bergner et al. (2002)

Rot 2b: Bergner et al. (2002)

Rot 3: Passrucker et al. (2003)

## SIMULATION AND EVALUATION OF RESULTS

### 3D Navier-Stokes Method

Details about the code used are given in Fritsch et al. (1997).

Geometry: The nominal clearance of 1% was used for the rotor tip gap. No cavities or fillets are resolved for the present investigations and the stator clearances have been neglected.

Grid Topology and CPU-Time: Simulations for datum design Rotor 1 utilised a composite H/O-grid with 155x33 nodes for the H-grid and 177x11 nodes for the O-grid in the S1-plane of the rotor; 65 nodes were used in the radial direction. A H-grid with 81x9x11 nodes was used to grid the tip gap. A comparable resolution in the stator yielded a combined total of 896,231 nodes. Simulations for other rotor designs show only minor departures in node numbers.

Turbulence Model: A high Reynolds'  $k-\epsilon$  model, resulting in a mean wall distance of  $y^+=25$  for rotor blade and casing and  $y^+=75$  for the hub, was used for economy. Resolution of stator flow was comparable to the rotor with the exception of the casing region, where the mean wall distance was increased to  $y^+=75$ . All simulations were run in a fully turbulent mode, with wall functions applied.

Boundary Conditions: ISA standard conditions with purely axial flow were assumed at the non-reflecting inflow boundary. The turbulence intensity measured in the experiment,  $Tu_1 = 1\%$ , was prescribed. The incoming casing boundary layer was prescribed via the total pressure profile.

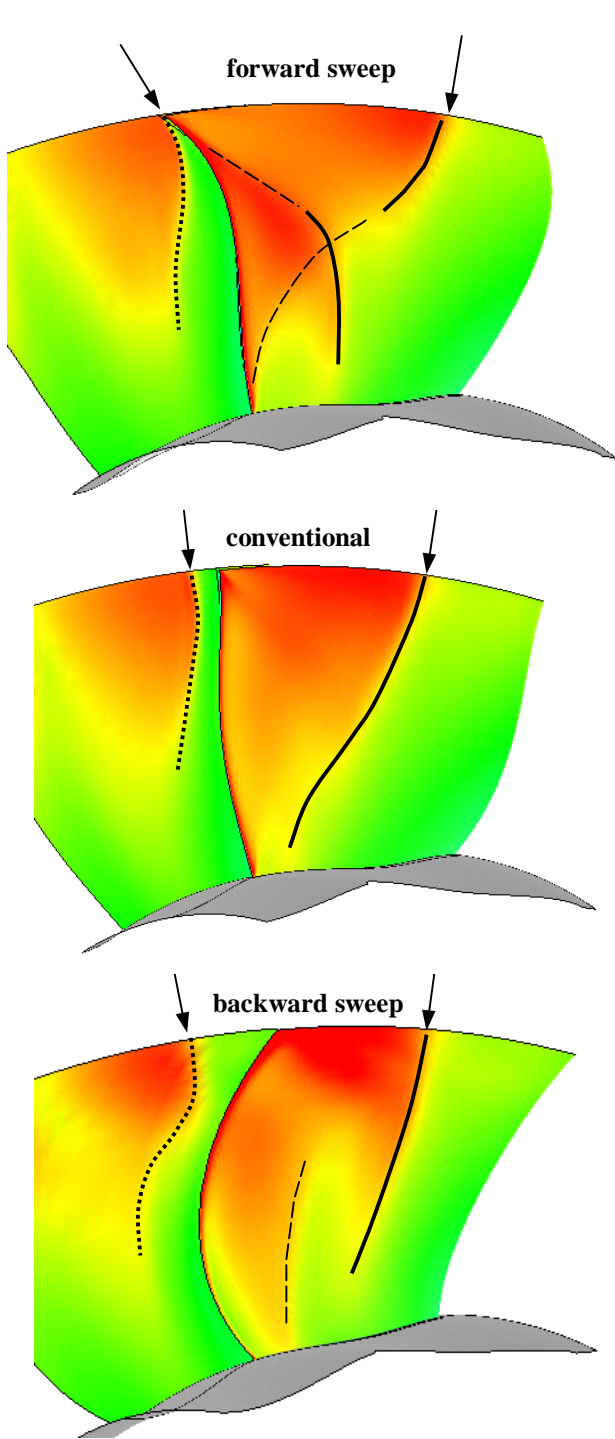


Fig. 3: Shock System on suction surface and in front of the leading edge, isentropic Mach numbers, view perpendicular to suction side at tip

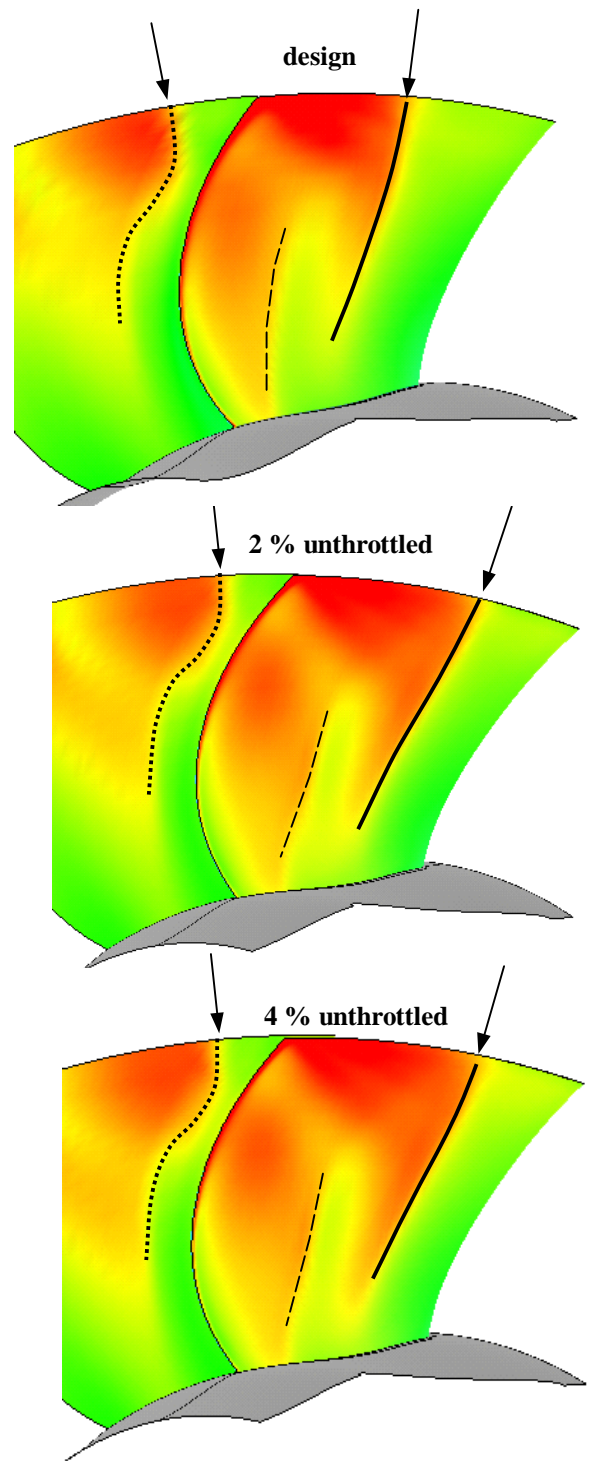
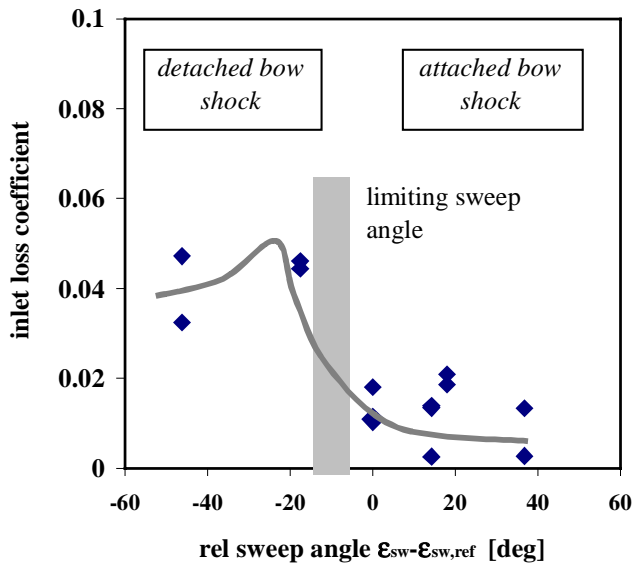


Fig. 4: Rotor 2 with unchanged bow shock pattern for unthrottled operation; isentropic Mach numbers, view perpendicular to suction side



**Fig. 5: Increase in inlet loss coefficient with negative sweep angles, streamline at 90% span**

#### Postprocessing

The pitch averaged flow in the meridional plane was obtained from 3D Navier-Stokes results using conservative variables (fluxes). Streamlines for the S2 averaged flow are then integrated.

#### ANALYSIS OF RESULTS

##### Shock system

The shock systems on the suction surface for 3 rotor designs with forward sweep, conventionally stacked and with backward sweep are given in Figure 3 at design conditions. To work out shock inclination at the casing the direction of the view is approximately perpendicular to the suction surface at the tip. Close to the leading edge an additional plane aligned in flow direction is used to visualize the bow shock wave.

Inside the blade passages all rotors show a weak oblique shock situation at the casing. Main shock locations are indicated by full black lines, dashed lines are drawn for secondary shocks. The most complex shock structure is found for the forward swept rotor 3 with 2 shocks to contribute to the diffusion process, while a double shock situation is found close to the hub of backward swept rotor 2.

The most interesting feature in Fig. 3 is the orientation of the bow shocks of the individual designs at the leading edge. For the conventionally (unswept) design and for the forward swept blade the bow shock follows the leading edge orientation at the casing. At the backward swept blade a flow deflection with attached bow shock is in conflict with the straight casing geometry. Here the bow

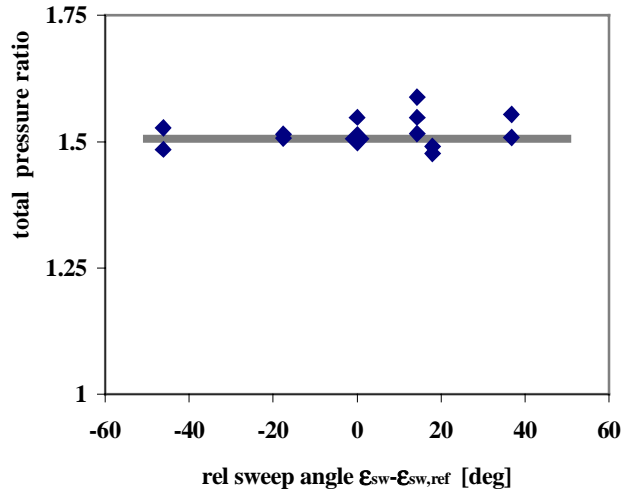


**Fig. 6: Profile section total pressure ratios for streamline at 90% span**

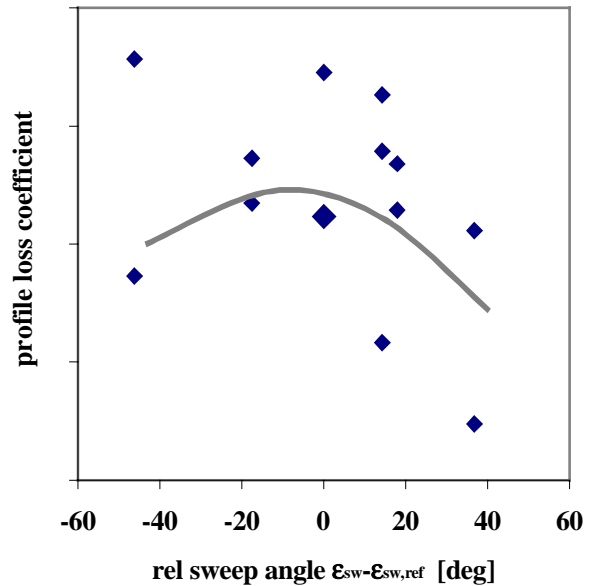


**Fig. 7: Profile section loss coefficient from eqn. (3), streamline at 90% span**

shock together with its pressure surface branch (reaching all across the blade passage on the suction surface) is pushed upstream. By that, in front of the leading edge a normal shock situation establishes and efficiency as well as mass transport at the rotor tip inlet are spoiled. This still holds true for lower back pressures and operating conditions below optimum efficiency., see fig. 4.

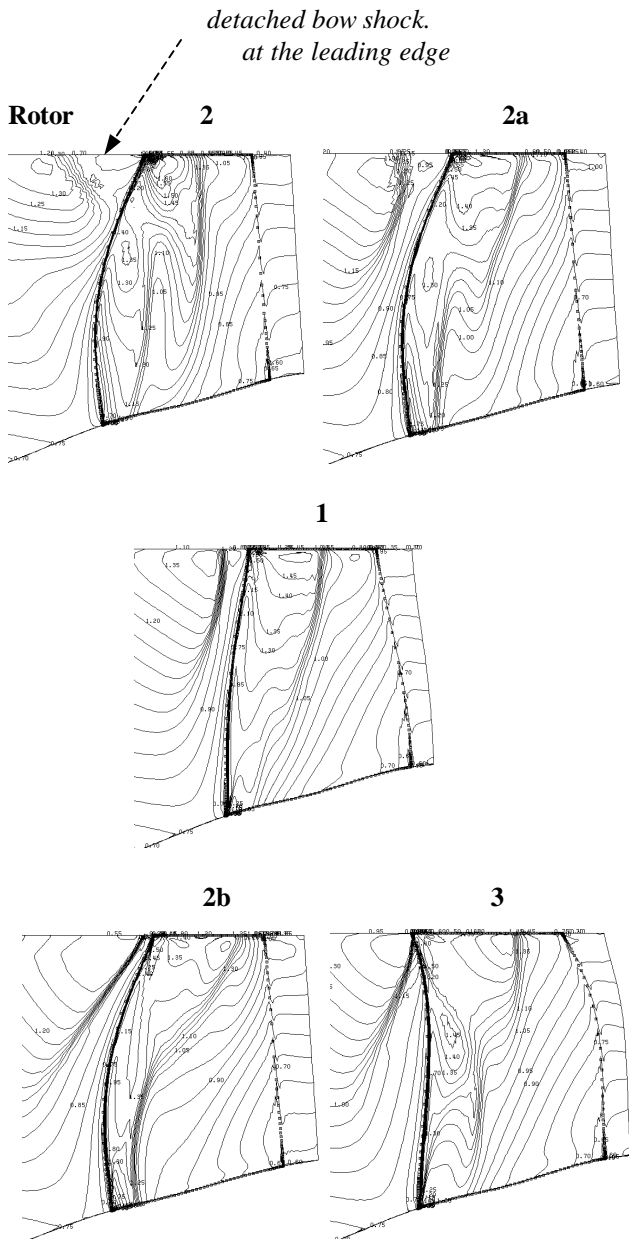


**Fig. 8: Bow shock situation from Mach number contours, meridional view for H-grid surfaces close to suction side, peak efficiency**

It can be deduced from Fig. 3 and 4 that for the shock casing interaction the region close to the leading edge seems to be more important than the interaction within the blade passage of the shock on the suction surface at casing. For a detailed analysis of shock leakage vortex interaction on rotor 1 see Hoeger et al. (1998) and (2000). To further analyze the impact of the leading edge sweep angle on the bow shock, 3D predictions for several rotor designs have been analyzed for a streamline (S2-

averaged) in the meridional plane outside the endwall boundary layer.

#### Streamline Section Loss Coefficient

A total pressure loss coefficient is defined on a streamline in the meridional plane, obtained from circumferentially averaged flow quantities intersecting the leading edge of the datum blade (rotor 1) in the tip region at 90% passage height. In the relative frame we have for the inlet:

$$\omega_{1,\text{inlet}} = (\text{Ptr}_1 - \text{Ptr}_{1e}) / (\text{Ptr}_1 - p_1) \quad (2)$$

as well as for the profile section:

$$\omega_{1,\text{prof}} = (\text{Ptr}_{1e} - \text{Ptr}'_{1e}) / (\text{Ptr}_1 - p_1) \quad (3)$$

The inlet loss coefficient from eqn. (2) contains the losses from the bow shock in front of the leading edge and the changes in relative total pressure from radial streamline displacement. The profile loss coefficient given in eqn. (3) uses an exit total pressure  $\text{Ptr}'_{1e}$ , which is corrected for radial changes in streamline position between rotor inlet and exit via a rotalpy expression.

In Fig. 5, 6 and 7 loss coefficients  $\omega_{1,\text{inlet}}$  and  $\omega_{1,\text{prof}}$  together with the corresponding pressure ratio is given for all 6 rotors at flow conditions close to optimum efficiency. A wide range of sweep angles is covered by the investigations. A decrease of relative total pressure in front of the rotor inlet plane is clearly visible with reduced leading edge sweep angle and with increased back pressure. With only little changes in pressure ratio, see Fig. 6, and a similar trend for the profile section loss coefficient, given in Fig. 7, the position of the bow shock is demonstrated not to be enforced by high loading levels or excessive losses of the profile section designs.

Limiting sweep angle: A limiting sweep angle may be deduced from the analysis, at which the bow shock at the casing is pushed upstream generating a normal shock/casing interaction. The predictions here show no further increases in both inlet loss coefficient  $\omega_{1,\text{inlet}}$  and profile section loss coefficient  $\omega_{1,\text{prof}}$ , see Fig. 5 and 7, although the total efficiency of the backswept rotor No. 2 decreases by a large amount, see Blaha et al. (2000).

In Fig. 8 the shock situation is given from Mach number contours close to the suction surface (meridional view of H-grid surface) for selected rotors at optimum efficiency. The detachment of the bow shock is demonstrated to be in line with the inlet total pressure drop given in Fig. 5. Applying circumferential lean to the axially backswept rotor 2, the effective sweep angle is increased, see eqn. (1). By that the flow situation is improved and an attached bow shock is gained again at the leading edge

for rotor 2b. The pronounced inclination of the shock system found for rotors 2a and 2b in Fig. 8 holds only true for the meridional view. A view normal to the suction surface (not given here) underlines the existence of a normal shock condition at the outer casing for backward swept designs. For forward swept designs, however, an inclined bow shock situation is clearly demonstrated to exist at the leading edge, see Fig. 3.

In general the limiting sweep angle may depend not only on blade geometry but on further design parameters, like e.g. operating condition, radial loading distribution, casing meridional angle and leading edge bluntness.

## CONCLUSIONS

Several rotor designs for the *Axial Single-stage Transonic Compressor Rig* of TU Darmstadt have been analysed on the basis of 3D Navier-Stokes predictions. The impact of the leading edge sweep angle on the shock system at inlet Mach numbers close to  $Ma_1=1.22$  was discussed. At 90% span the forward swept blade designs showed the lowest relative total pressure drop at the rotor inlet and a fully attached in the radial direction oblique bow shock at the casing. For backward swept designs a lower limiting sweep angle was found at which the bow shock can no longer remain attached to the leading edge but is pushed upstream causing efficiency penalties and lower stability margins. A combination of high axial backward sweep with circumferential lean, however, allowed for attached bow shocks too. Further benefits are expected for this backward swept/ forward leaned rotor (rotor No. 2b) by redesigning with 3D Navier-Stokes methods.

## REFERENCES

Bergner, J., Hennecke, D. K., Hoeger, M., Engel, K. „Darmstadt Rotor No. 2 - part II Design of leaned Rotor Blades“, ISROMAC 9, Honolulu, Hawaii, USA, Feb. 10-14, 2002.

BlaHa, C., Kablitz, S., Hennecke, D., Schmidt-Eisenlohr, U., Pirker, K., Haselhoff, S., 2000. „Numerical Investigation of the Flow in an Aft-Swept Transonic Compressor Rotor“, Proc. of the ASME Turboexpo 2000, paper 2000-GT-04090.

Bölcs, A., Suter, P., 1986, “Transsonische Turbomaschinen”, Reihe Wissenschaft und Technik, Verlag G. Braun, Karlsruhe.

Cybyk, B.Z., Car, D., Hah, C., 1997, “Impact of CFD on Test and Evaluation at the Compressor Research Facility“, AIAA 97-2881.

Denton, J. D., 1999. „Exploitation of 3D Flow in Turbomachinery Design“, in: Van den Braembusche, R. A., (Editor), „Turbomachinery Blade Design Systems“, VKI

Lecture Series 1999-02, von Karman Institute for Fluid Dynamics.

Fritsch, G., Hoeger, M., Blaha, C., Bauer, D., 1997, “Viscous 3D Compressor Simulation on Parallel Architectures“, AIAA 97-2876.

Hah, C., Puterbaugh, S. L., Wadia, A. R., 1998. „Control of Shock Structure and Secondary Flow Field inside Transonic Compressor Rotors through Aerodynamic Sweep“, ASME paper 98-GT-561.

Hoeger, M., Fritsch, G., Bauer, D., 1998, “Numerical Simulation of the Shock-Tip Leakage Vortex Interaction in a HPC Front Stage“, ASME-Paper 98-GT-261.

Hoeger, M., Lahmer, M., Dupslaff, M., Fritsch, G., 2000, “A Correlation for Tip Leakage Blockage in Compressor Blade Passages“, ASME Journal of Turbomachinery, Vol. 122, pp. 426.

Kablitz, S., Bergner, J., Hennecke, D. K., Beversdorff, M., Schodl, R. „Darmstadt Rotor No. 2 - part III Experimental Analysis of an Aft-Swept Axial Transonic Compressor Stage“, ISROMAC 9, Honolulu, Hawaii, USA, Feb. 10-14, 2002.

Passrucker, H., Engber, M., Kablitz, S., Hennecke, K., 2003, The Effect of Forward Sweep in a Transonic Compressor Rotor, 5<sup>th</sup> European Conference on Turbomachinery, Fluid Dynamics and Thermodynamics, Conference Proceedings, pp. 141.

Pirker, K., Frischbier, J., „Darmstadt Rotor No. 2 - part I Design and Stress Analysis of a One Stage Transonic Composite Compressor“ ISROMAC 9, Honolulu, Hawaii, USA, Feb. 10-14, 2002.

Schreiber, H. A., „Shock losses in Transonic and Supersonic Compressor Cascades“, VKI-Lecture Series LS 88-03, „Transonic Compressors“, Brussels, Belgium, Feb. 1-5. 1988.